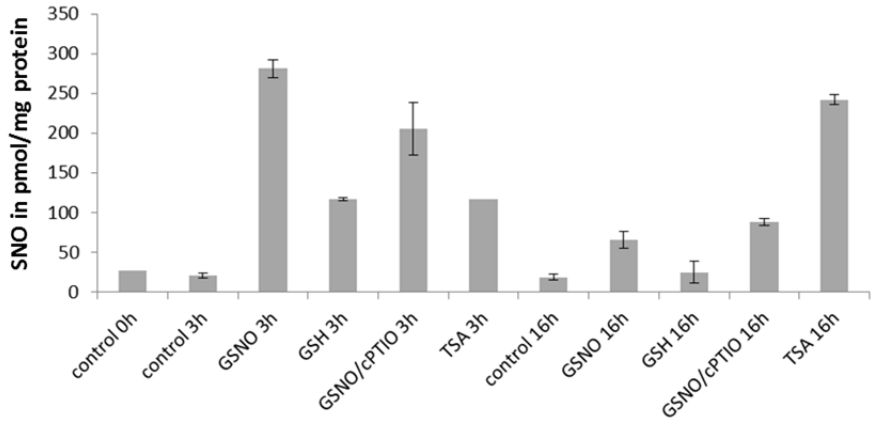

Supplemental Figure 1: **S-Nitrosothiol levels in liquid grown *Arabidopsis* seedlings after GSNO, GSH, GSNO/cPTIO, TSA and water (control) treatment.** Seedlings were treated with 250 µM GSNO, 250 µM GSH, 250 µM GSNO / 500 µM cPTIO, 5 µM TSA or water (control) and total S-nitrosothiol levels were determined after 3h and 16h. SNOs were reduced with triiodide and the emitted NO was photochemically detected by its reaction with ozone.

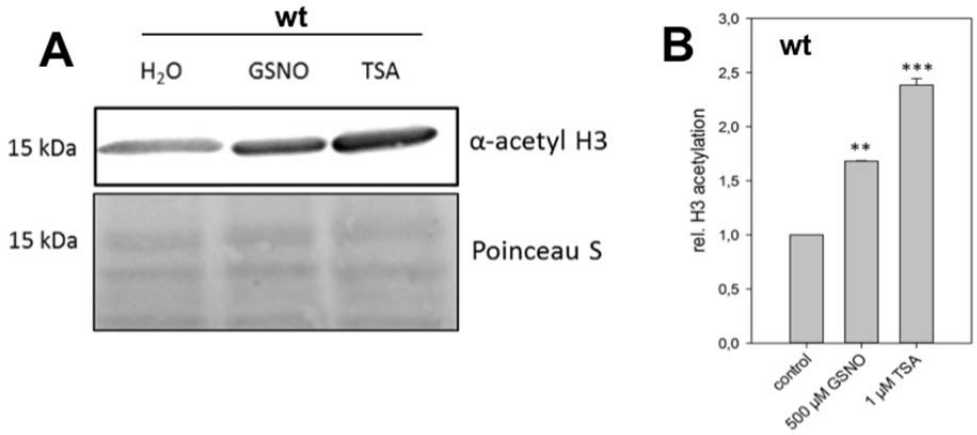

Supplemental Figure 2: GSNO increases H3ac in *Arabidopsis* suspension cells. A) Western-Blot analysis of GSNO- and TSA-treated wild-type cells. Nuclear extracts were separated by SDS-PAGE and blotted. The membrane was probed with an anti-acetyl H3 primary antibody and a secondary antibody coupled to HRP. Shown is one representative experiment. B) Quantification of A. Signal intensity was determined with Image J software. Shown is the mean ± SEM of three experiments. **P < 0.01, ***P < 0.001, student´s t-test.

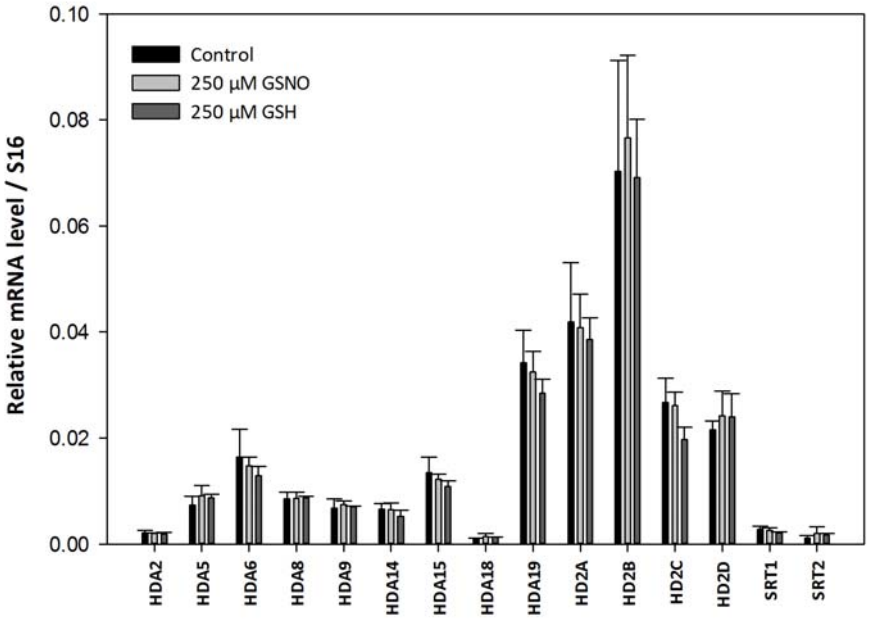

Supplemental Figure 3: mRNA levels of HDACs after GSNO and GSH treatment. mRNA levels were determined by qPCR using gene-specific primer pairs. Values are expressed as mean ± SD of three independent experiments, normalized to S16 mRNA level.

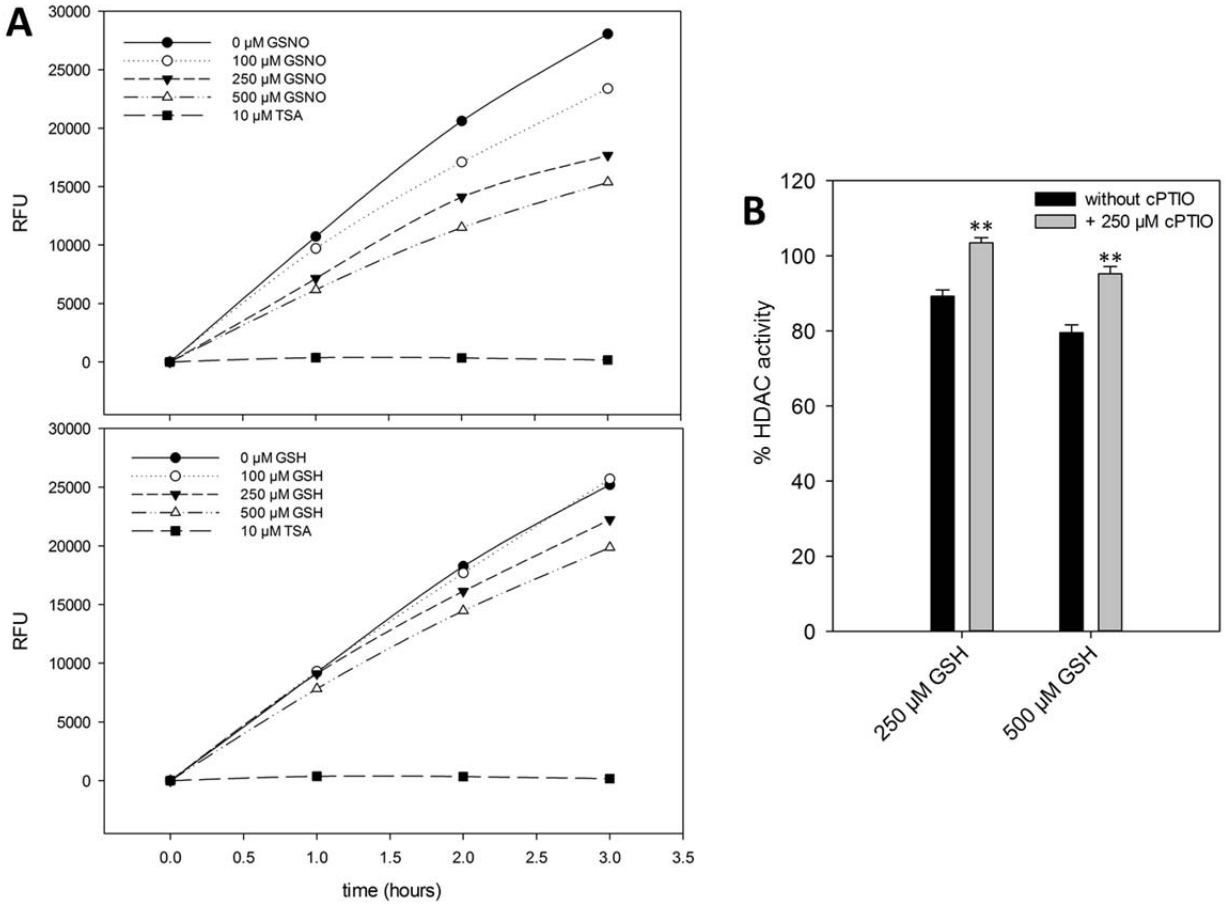

Supplemental Figure 4: Inhibition of HDAC activity by GSH. A) Protoplasts were stimulated with 100 µM, 250 µM and 500 µM GSNO or GSH and HDAC activity was recorded for 3h. Specificity of the assay was demonstrated by using TSA, a strong HDAC inhibitor. Shown is one representative experiment out of two. B) HDAC inhibition by GSH can be prevented by cPTIO. Protoplasts were preincubated with cPTIO and then stimulated with 250 µM and 500 µM GSH. HDAC activity was recorded after 2h. Values are normalized to water treated (- cPTIO) or cPTIO treated (+ cPTIO) protoplasts. Shown is the mean ± SEM of three independent protoplast preparations. **P < 0.01, student´s t-test.

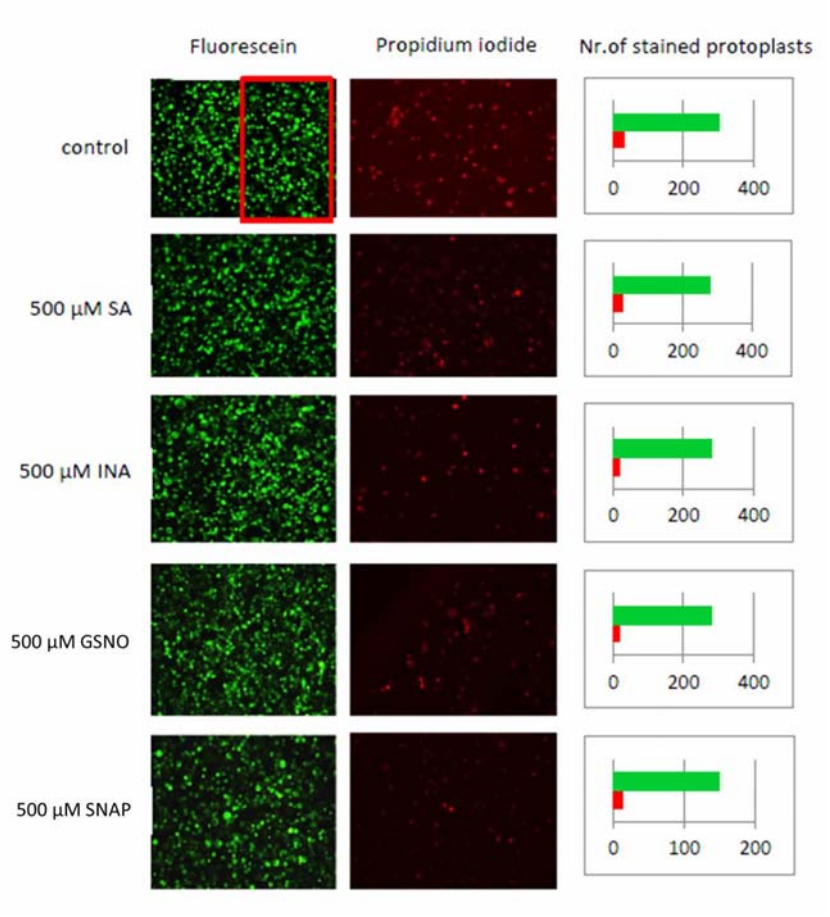

Supplemental Figure 5: Viability of protoplasts after SA, INA, GSNO and SNAP treatment. Protoplasts were stained simultaneously with fluorescein diacetate and propidium iodide. Viable (accumulation of fluorescein in the cytosol, green) and non - viable (accumulation of propidium iodide in the nucleus, red) cells were counted in one half of the images (red square), the respective numbers are depicted in the diagrams on the right. Green bars represent viable, red bars represent non-viable cells.

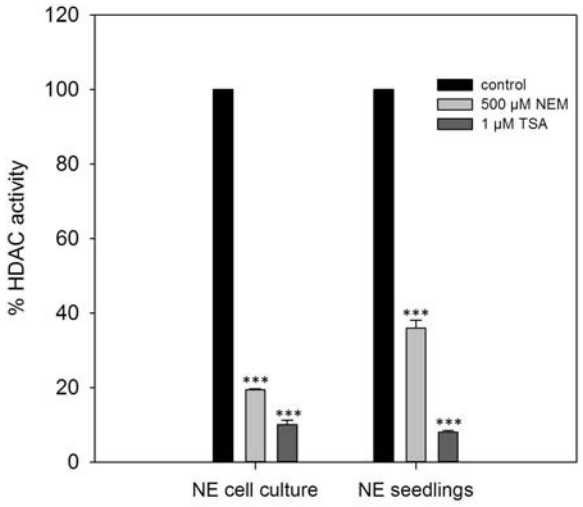

Supplemental Figure 6: Inhibition of nuclear HDAC activity by NEM and TSA. Nuclear extracts (NE) from *Arabidopsis* suspension cells or liquid grown seedlings (7 days) were treated with 500 µM NEM. 1 µM TSA was used as a positive control. Values are mean ± SEM of three independent preparations of nuclear extracts and normalized to control treatment. ***P < 0.001, Student´s t-test.

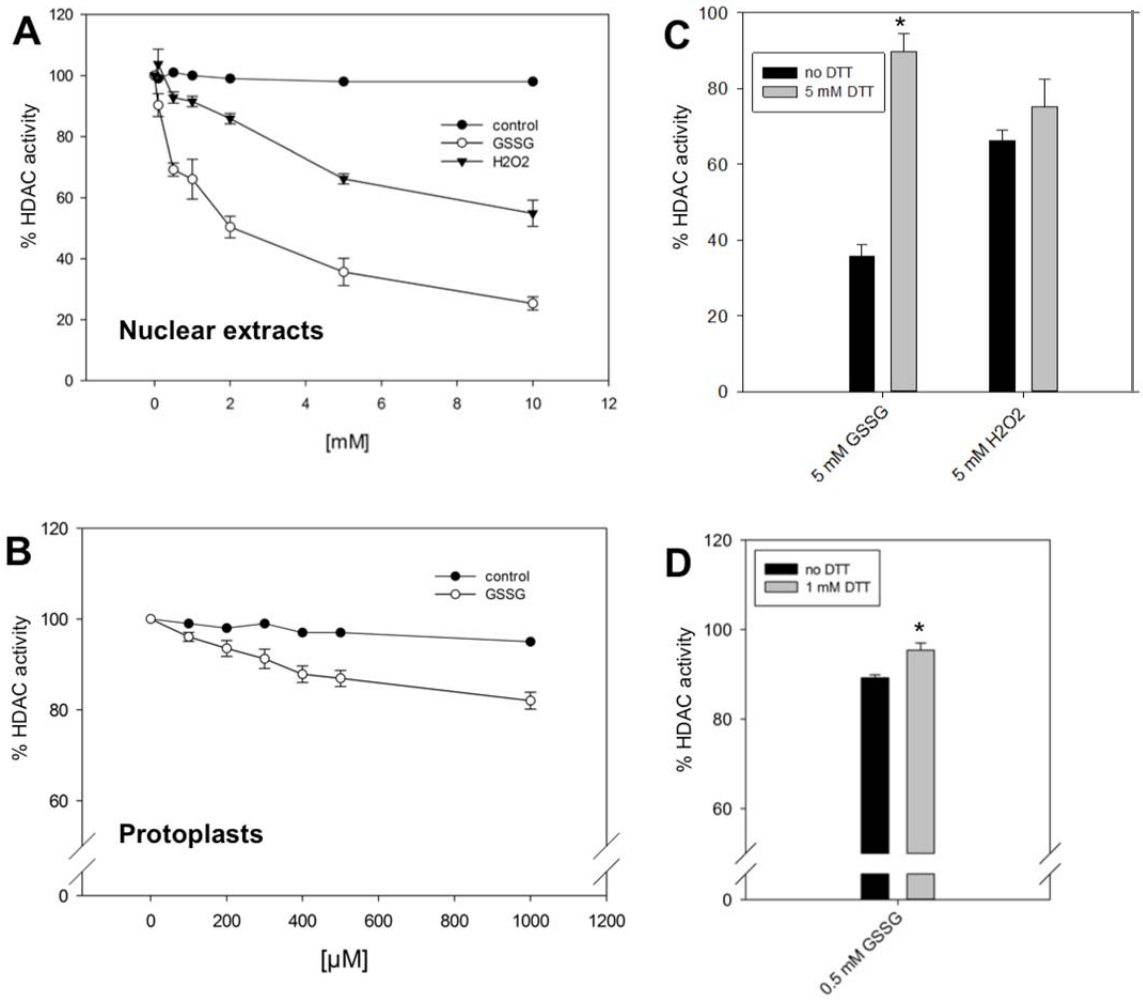

Supplemental Figure 7: Inhibition of HDAC activity by GSSG and H_2O_2. A) Nuclear extracts from *A. thaliana* cell culture were incubated with different concentrations of GSSG and H_2O_2. B) Protoplasts from *A. thaliana* cell culture were treated with GSSG. C and D) DTT restored HDAC activity after GSSG but not H_2O_2 treatment. Nuclear extracts and protoplasts were incubated with DTT after GSSG and H_2O_2 addition. Values are expressed as percentage of HDAC activity in untreated nuclear extracts or protoplasts. Values are mean ± SEM of three independent preparations of nuclear extract or protoplasts. * $P < 0.05$, student´s t-test.

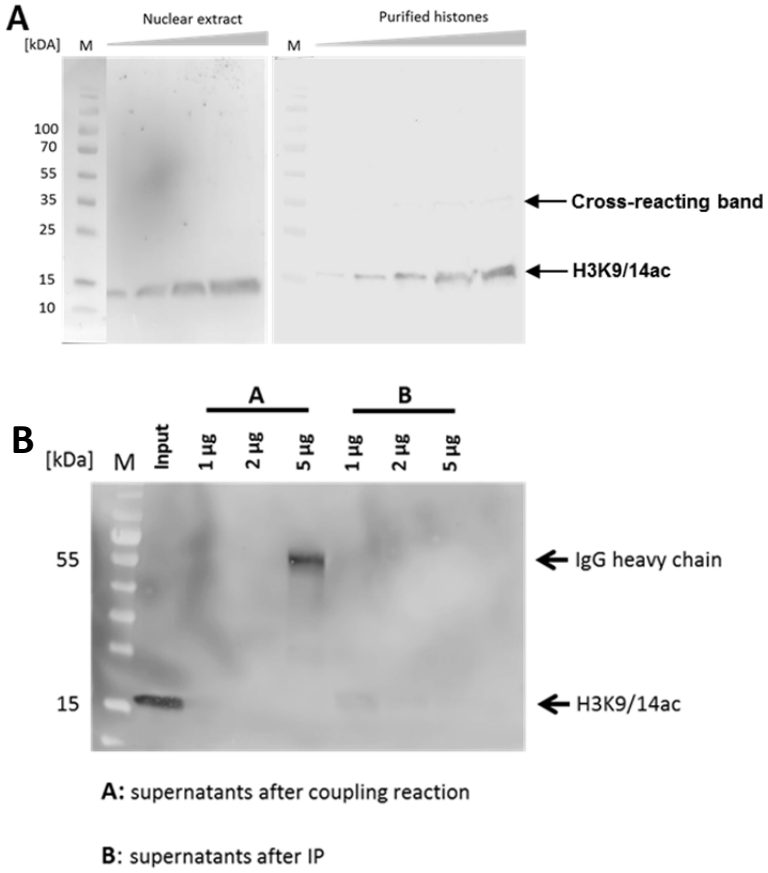

Supplemental Figure 8: **Antibody quality control and titration**. Different quantities of nuclear extracts and purified histones were separated by 12 % SDS-PAGE, blotted on nitrocellulose and probed with an anti-H3K9/14ac antibody (Diagenode). Secondary antibodies were anti-rabbit-IgG-HRP (Promega, nuclear extracts) and anti-rabbit-AP (Promega, purified histones). The antibody was highly specific and only very weakly cross-reacted with H1, fulfilling the ENCODE criteria for ChIP-seq antibodies. B) Titration experiment to determine the optimal amount of antibody. 1, 2 and 5 µg of anti-H3K9/14ac antibody were coupled to magnetic beads and aliquots of the supernatants after the coupling reaction (to assess the success of the coupling reaction) as well as after the immunoprecipitation (to check whether all antigen was immunoprecipitated) were probed with the same antibody. Sheared chromatin (input) was used as positive control. In these experiments chromatin was isolated from 2 g of starting material, for subsequent experiments only 1 g of material was used. Therefore, although a slight band is visible in lane 6, 1 µg of antibody was sufficient to immunoprecipitate all of the antigen present in the sample prepared from 1 g of tissue.

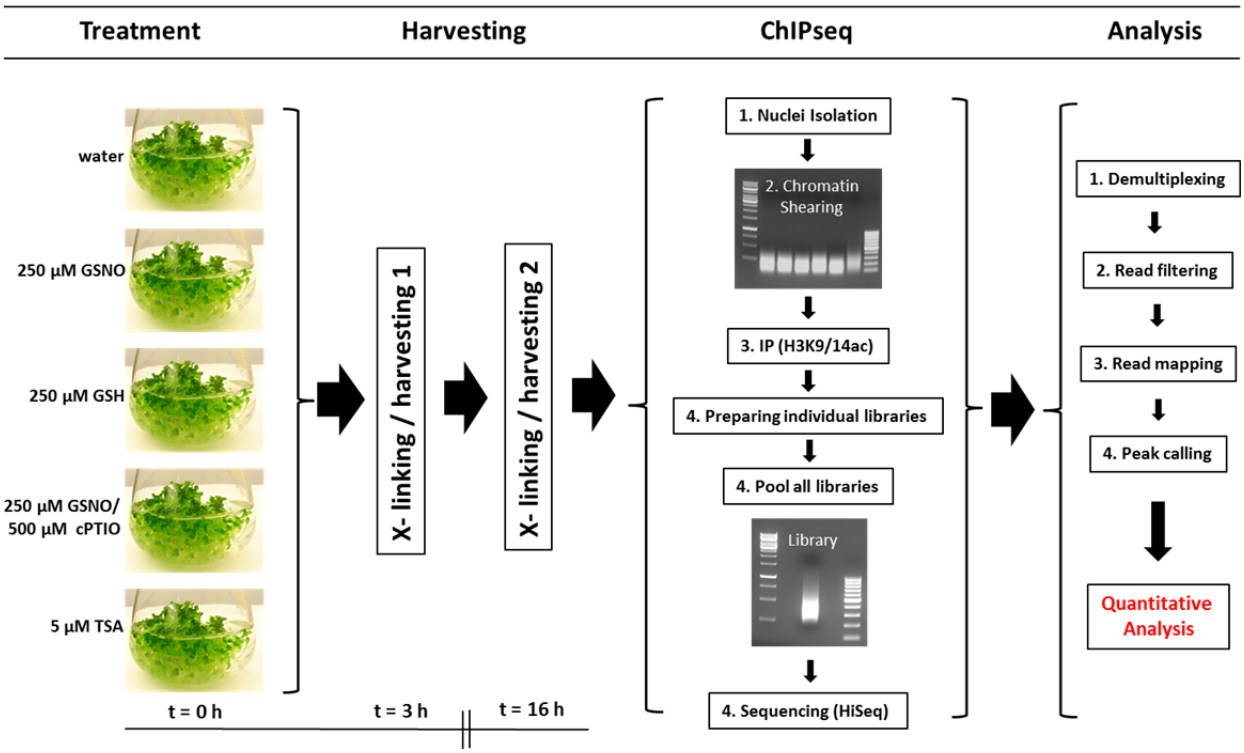

Supplemental Figure 9: Workflow to quantitatively determine differences in the H3K9/14ac pattern after GSNO, GSH, GSNO/cPTIO and TSA treatment. Liquid grown *Arabidopsis* seedlings were treated with water (control), 250 µM GSNO, 250 µM GSH, 250 µM GSNO / 500 µM cPTIO and 5 µM TSA. 3h and 16h later seedlings were crosslinked and harvested. ChIP was done with an antibody directed against H3K9/14ac. The experiment was performed in two biological replicates. For each sample (in total 20) 1 ng of the immunoprecipitated DNA and 1 ng of the corresponding input DNA was used to prepare indexed libraries. All libraries were pooled and sequenced. Reads were then demultiplexed, filtered (only uniquely mapped reads were kept) and mapped back to the *Arabidopsis* genome (TAIR9). Finally, H3K9/14ac peaks were identified and differences in the H3K9/14ac pattern across the different treatments were quantified.

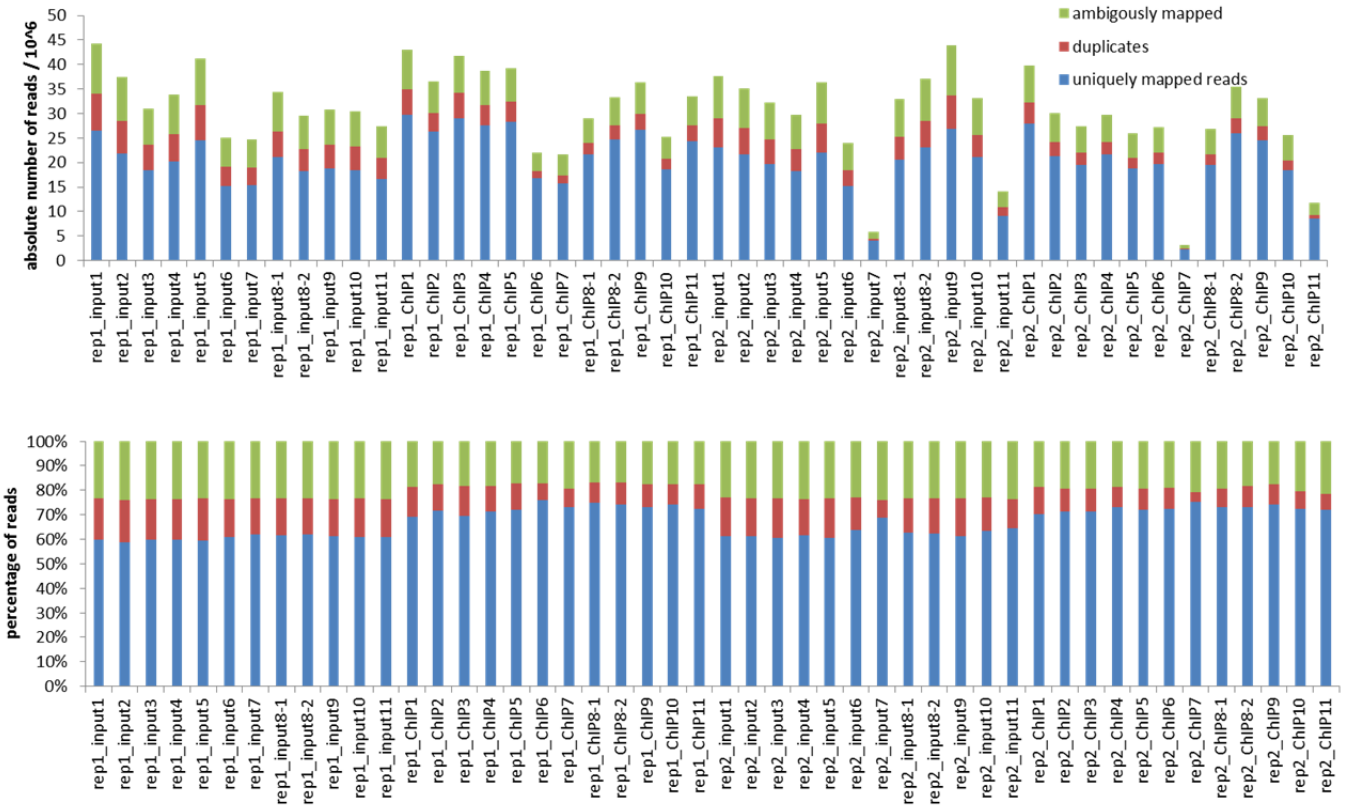

Supplemental Figure 10: **Summary of read mapping**. Raw reads generated by an Illumina HiSeq 2500 were aligned to the *Arabidopsis* reference genome (TAIR10) using the mapping tool of the clc genomics workbench (Qiagen) with default settings. Reads that mapped to more than one position and duplicate reads originating from PCR artefacts were excluded from further analysis. 15 - 30 million uniquely mapping high quality reads per sample were obtained. Due to the low number of reads, rep2_input7 and rep2_ChIP7 (corresponding to control_16h) and rep2_input11 and rep2_ChIP11 (corresponding to TSA_16h) could not be used for further analysis.

treatment	name	# reads	# peaks	RSC	NSC	peaks/reads
control t = 0	rep1_ChIP1	29683571	12784	1.009	1.131	0.000431
control t = 3	rep1_ChIP2	26258106	13882	1.060	1.198	0.000529
GSNO t = 3	rep1_ChIP3	29101321	13521	1.055	1.174	0.000465
GSH t = 3	rep1_ChIP4	27597269	12979	1.038	1.174	0.000470
cPTIO t = 3	rep1_ChIP5	28241039	13573	1.054	1.185	0.000481
TSA t = 3	rep1_ChIP6	16785680	13627	1.021	1.242	0.000812
control t = 16	rep1_ChIP7	15793934	6838	1.006	1.176	0.000433
GSNO t = 16	rep1_ChIP8-1	21722687	13484	1.068	1.241	0.000621
GSNO t = 16	rep1_ChIP8-2	24695272	14182	1.072	1.232	0.000574
GSH t = 16	rep1_ChIP9	26653757	13802	1.056	1.187	0.000518
cPTIO t = 16	rep1_ChIP10	18674559	10701	1.010	1.197	0.000573
TSA t = 16	rep1_ChIP11	24318293	14758	1.005	1.149	0.000607
control t = 0	rep2_ChIP1	27871262	439	0.897	1.084	0.000016
control t = 3	rep2_ChIP2	21377496	9136	0.986	1.157	0.000427
GSNO t = 3	rep2_ChIP3	19585686	7885	0.993	1.163	0.000403
GSH t = 3	rep2_ChIP4	21740591	11754	1.042	1.207	0.000541
cPTIO t = 3	rep2_ChIP5	18765809	8657	1.014	1.192	0.000461
TSA t = 3	rep2_ChIP6	19730422	11119	0.973	1.170	0.000564
control t = 16	rep2_ChIP7	2331035	1200	0.391	1.203	0.000515
GSNO t = 16	rep2_ChIP8-1	19546017	8572	0.999	1.167	0.000439
GSNO t = 16	rep2_ChIP8-2	25941867	9316	0.976	1.120	0.000359
GSH t = 16	rep2_ChIP9	24542001	13436	1.070	1.226	0.000547
cPTIO t = 16	rep2_ChIP10	18479068	6031	1.016	1.179	0.000326
TSA t = 16	rep2_ChIP11	8469745	385	0.717	1.119	0.000045

Supplemental Figure 11: Summary of peak calling parameters. The number of called peaks correlates with the number of reads in each sample. The relative strand cross-correlation (RSC) describes the ratio between the fragment-length peak and the read-length peak in the cross-correlation plot. Successful ChIP-experiments have RSC values greater than 0.8. The normalized strand coefficient describes the ratio between the fragment-length peak and the background cross-correlation values. This value should be greater than 1.05 for ChIP-seq experiments (CLC genomics workbench).

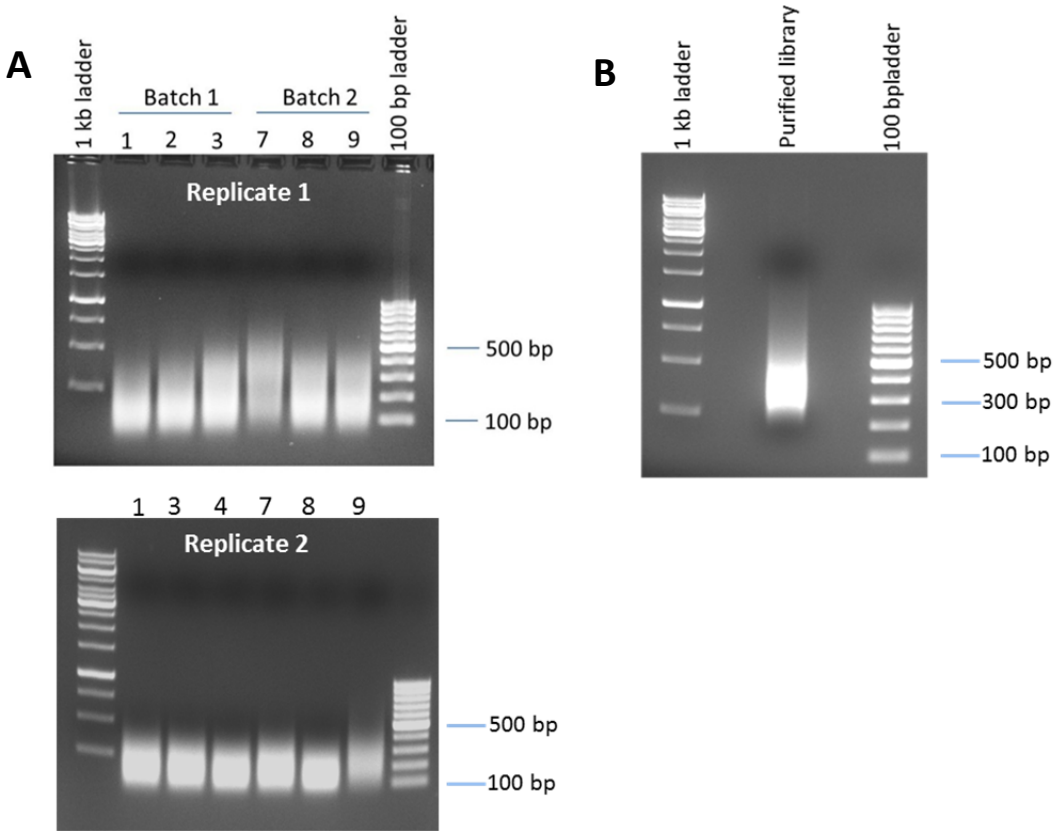

Supplemental Figure 12: Shearing and library preparation. A) Aliquots of sheared chromatin were separated on a 1.5% agarose gel and stained with ethidium bromide, revealing that the length of the fragments was between 100 and 500 bp, with a maximum at 200 bp. This length distribution was optimal for ChIPseq (Landt et al., 2012). B) An aliquot of the final pooled library (consisting of 48 individual libraries, see Fig.1, additional technical replicates from GSNO treated sample) was separated on a 1.5% agarose gel and stained with ethidium bromide. Fragments had an average length of around 350 bp (200 bp DNA fragment + 150 bp adapters), demonstrating that library preparation was successful.

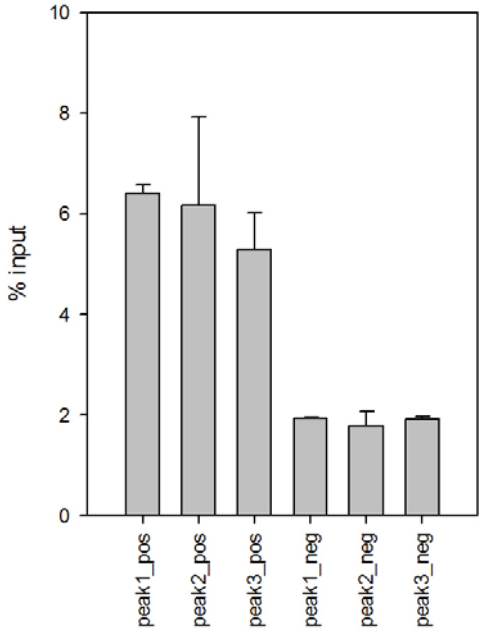

Supplemental Figure 13: Verification of Peak calling. In order to validate the peak calling algorithm, three predicted peak (Peak_pos) and adjacent non-peak (peak_neg) regions were chosen and primer sets to amplify these regions by qPCR were designed.

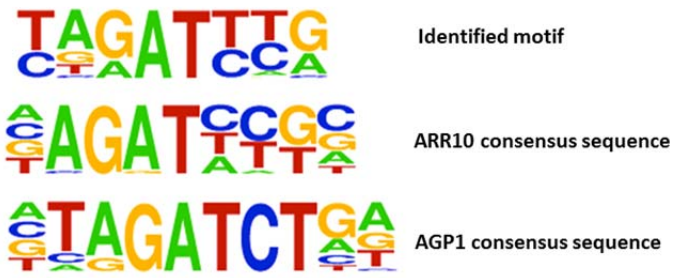

Supplemental Figure 14: **Motif analysis of H3K9/14ac peak regions**. Shown is the most significant motif (P-value = E-168) and the ARR10 and AGP1 consensus sequences for comparison. The identified motif strongly resembles the consensus sequences of both transcription factors. The figure was prepared using the ChIPseek software portal (http://chipseek.cgu.edu.tw/).

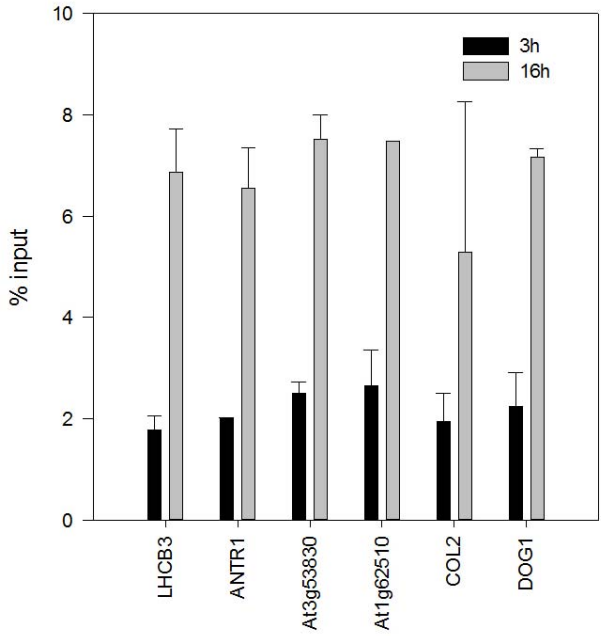

Supplemental Figure 15: Verification of the quantitative analysis (DiffBind) by ChIP-qPCR. To verify the quantitative analysis, differentially regulated peaks in control_3h vs. control_16h were identified. The predicted sites were then confirmed using qPCR and peak-specific primer sets. All of the six candidates tested showed increased H3K9/14ac levels after 16h of treatment – as determined by DiffBind. Values are expressed as % of the input. Shown is the data for two biological replicates, with two technical replicates each.

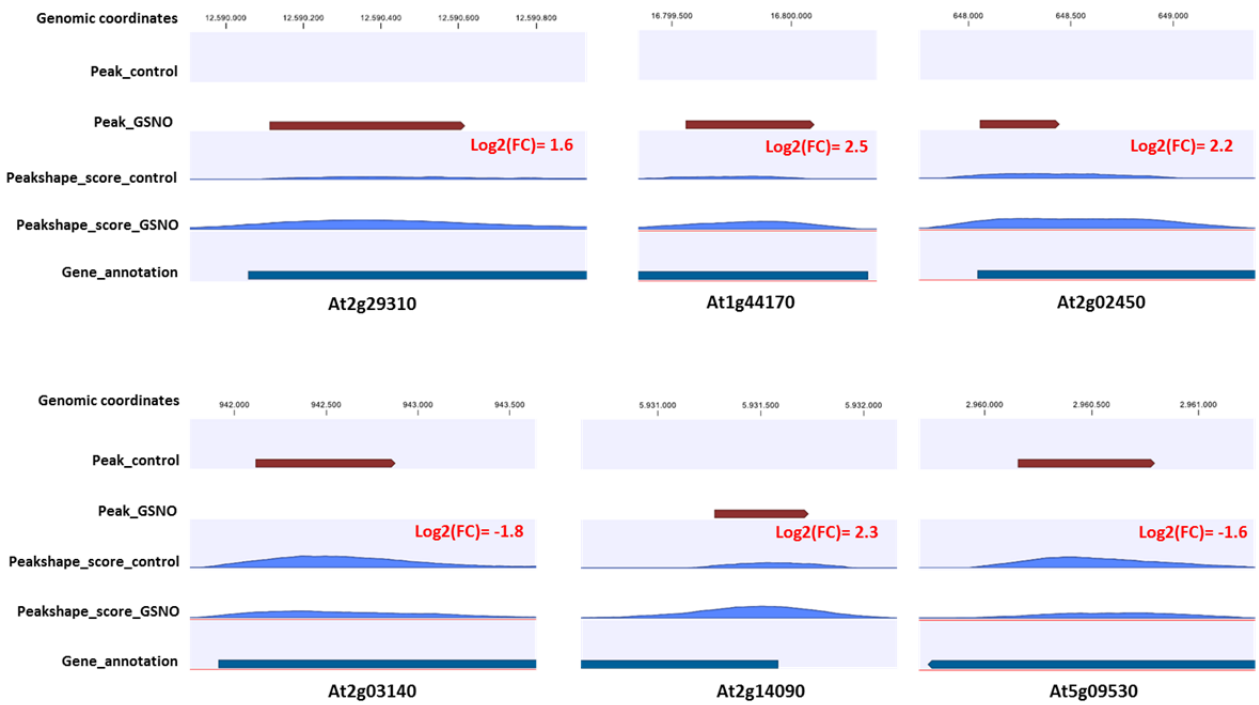

Supplemental Figure 16: CLC-genome browser snapshots of representative GSNO-regulated H3K9/14ac sites. Brown arrows indicate whether a peak was found in this region during peak-calling for water (second line: Peak_control) or GSNO (third line: Peak_GSNO) treatment. The peak-shape score (fourth and fifth line) is a measure for how well the read distribution fits to the peak shape filter applied for peak identification. The peak-shape score correlates with the read density in the corresponding region. The numbers in red indicate the predicted log2 fold change (treatment-control) as computed by DiffBind.

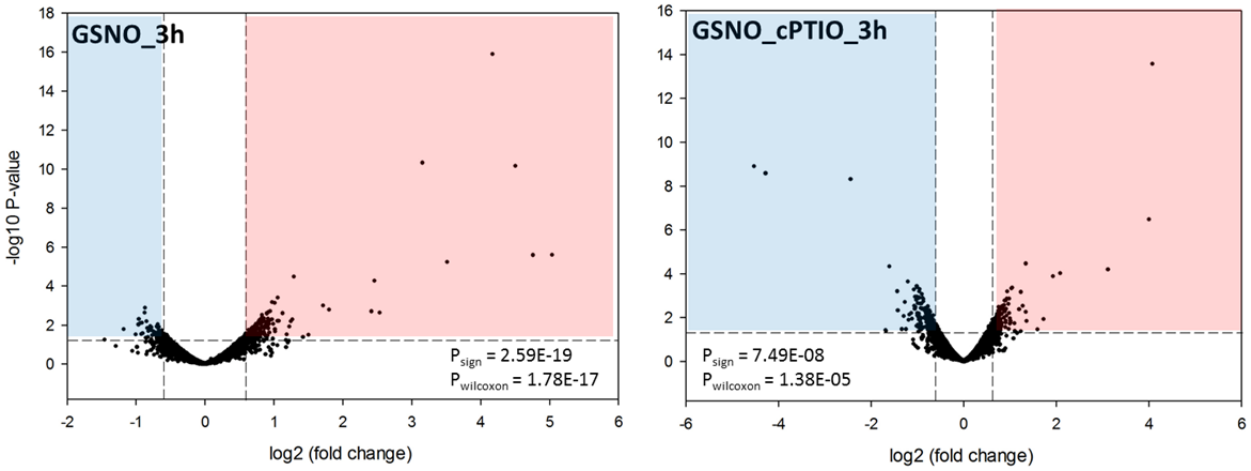

174

175 **Supplemental Figure 171: cPTIO reduces the number of hyperacetylated H3K9/14ac sites**
176 **after 3h of GSNO treatment.** Volcano plots in which the –log10(P-value) of each analyzed
177 H3K9/14ac site is plotted versus the corresponding log2(fold change (treatment over control)).
178 The horizontal dashed line corresponds to a P-value of 0.05, the two vertical dashed lines mark
179 fold changes of ± log2(1.5). To test for significant differences in the number of peaks with
180 enhanced or decreased H3K9/14ac among the peaks with p-values < 0.05, sign-tests were
181 performed (P_{sign}). To test whether peaks with increased H3K9/14ac show higher absolute
182 log2(fold changes) compared to peaks with decreased H3K9/14ac, Wilcoxon signed rank tests
183 were performed ($P_{wilcoxon}$).

184

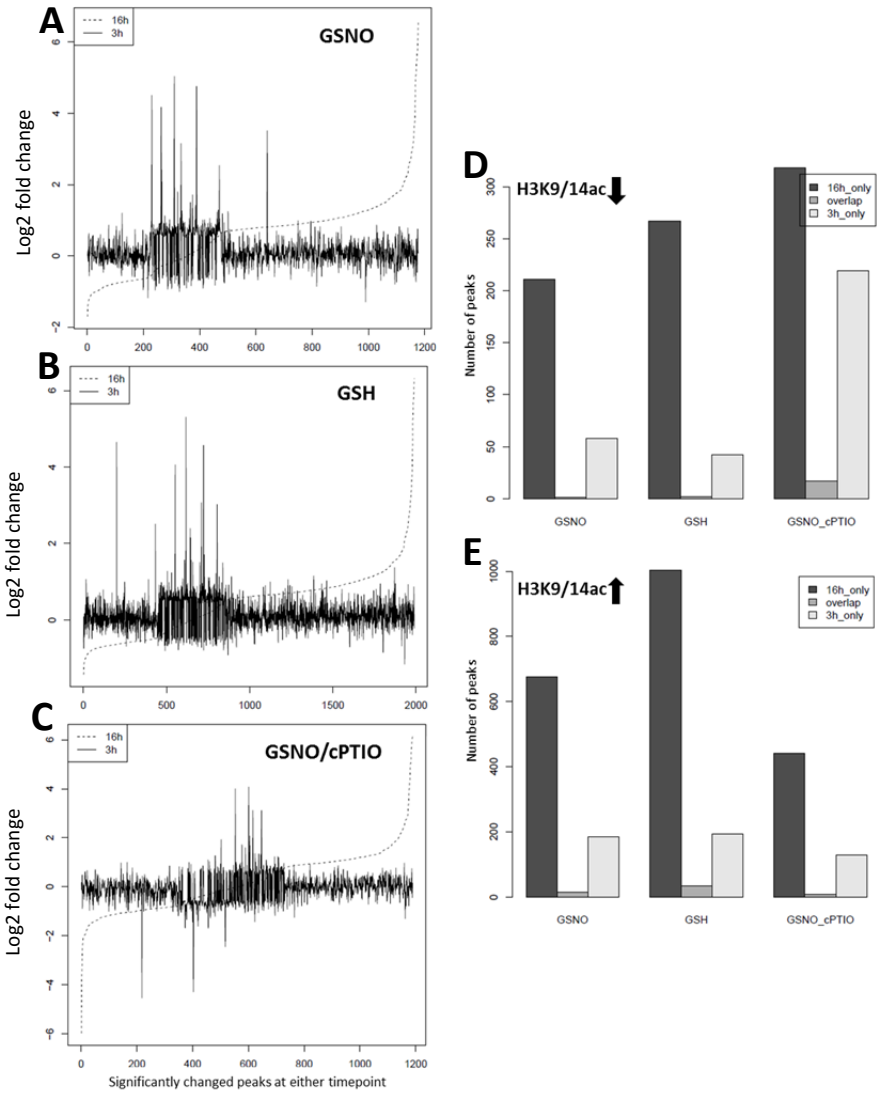

Supplemental Figure 18: Time point comparison of GSNO -, GSH - and GSNO/cPTIO - induced H3K9/14ac changes. A – C: Peaks showing altered H3K9/14ac with $P < 0.05$ in the 3h or 16h time point were combined and sorted for increasing log2(FC) in the 16h time point (dotted line). The solid line reflects the log2(FC) for the corresponding peaks after 3h of treatment. These line-plots indicate that peaks which show strong H3K9/14ac changes in either time point are not or only slightly regulated at the other time point arguing for substantially different responses after 3h and 16h of treatment. D and E: Number of significantly changed H3K9/14ac peaks ($P<0.05$), which are found after 16h or 3h only (dark grey and light grey bars) or at both time points (grey bars) separated for peaks showing enhanced (E) or decreased H3K9/14ac (D).

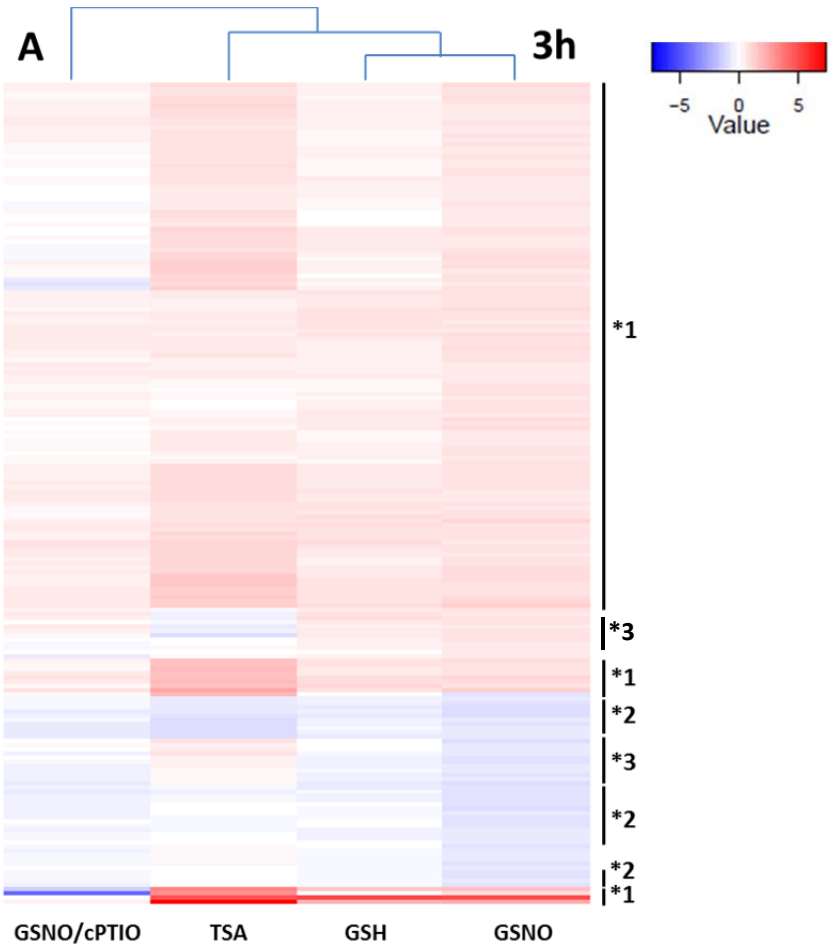

Supplemental Figure 19: Comparison of NO-induced H3K9/14ac changes with the TSA treatment. NO-regulated H3K9/14ac sites were identified by comparison of the GSNO and GSNO/cPTIO treatments (see text for details). Each line represents one NO-regulated H3K9/14ac site. The log2(FC) (treatment over control) of H3K9/14ac of these sites is shown for the GSNO, GSH, TSA and GSNO/cPTIO treatments. *1: sites which show enhanced H3K9/14ac in response to NO and TSA treatment. 2*: sites which show decreased H3K9/14ac in response to NO and TSA treatment. *3: sites which are oppositely regulated in response to NO and TSA treatment.

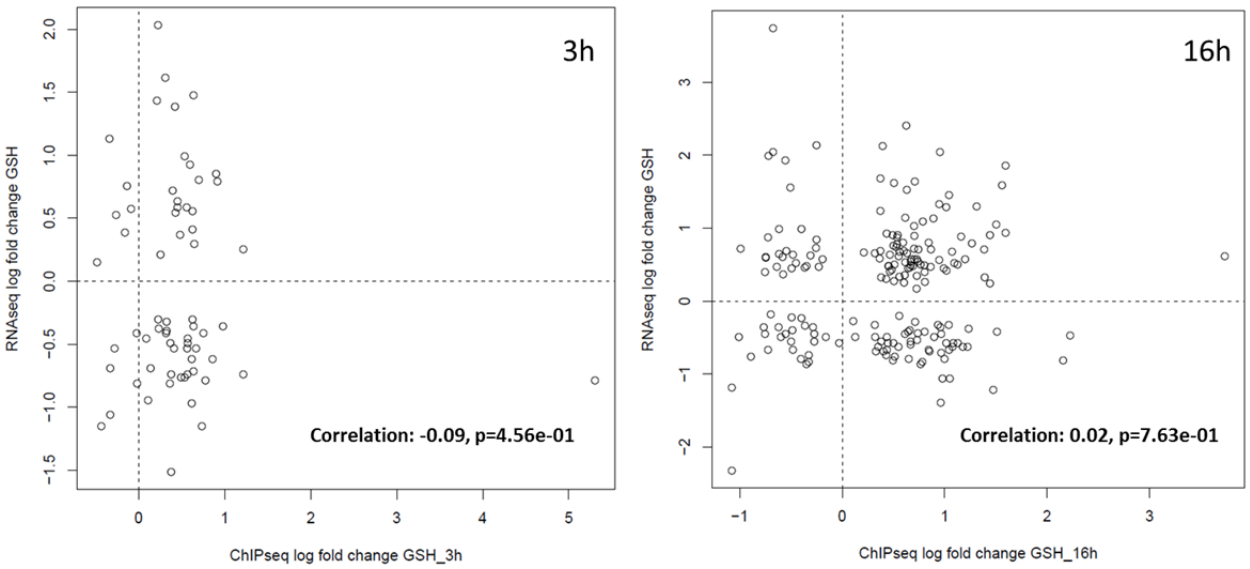

209

210 **Supplemental Figure 20: Correlation analysis of GSH-mediated changes of H3K9/14ac and**
211 **gene expression.** Correlation analysis of genes displaying GSH-mediated H3K9/14ac changes
212 after 3h (A) or 16h (B) and GSH-induced transcriptional changes (after 3h), based on a recently
213 published RNAseq dataset (Begara-Morales et al., 2014).

214

215

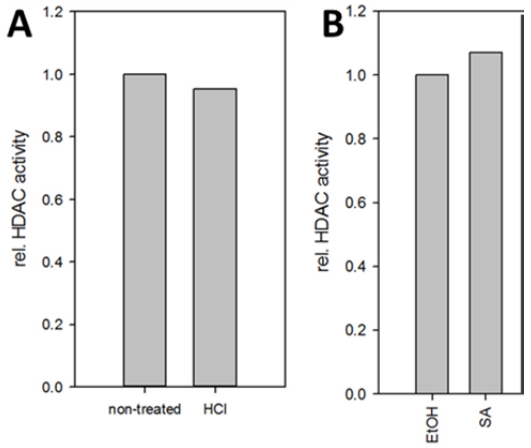

216

217 **Supplemental Figure 21: HDAC assay control experiments.** A) Protoplasts were incubated
218 with diluted HCl at a pH similar to a SA/INA solution and HDAC activity was determined. B)
219 Nuclear extracts were incubated with SA and HDAC activity was measured. The experiment was
220 repeated once with similar results.

Supplemental Table 1: GO-enrichment analysis for genes displaying NO-regulated H3K9/14ac. GO terms with P-values < 0.01 are listed together with the corresponding ID, P-value and FDR adjusted P-value (FDR). The "set" column indicates whether the GO term was enriched among genes displaying increased histone acetylation after 3h (3h_up) or 16h (16h_up). GO terms marked in bold belong to the category "biological process". All other terms belong to "molecular function".

GO term	GO ID	Set	P-value	FDR
small conjugating protein ligase activity	GO:0019787	16h_up	0.0012	0.411
sulfur compound binding	GO:1901681	16h_up	0.0037	0.641
ligase activity	GO:0016874	16h_up	0.0061	0.683
carbohydrate kinase activity	GO:0019200	16h_up	0.0082	0.683
defense response	**GO:0006952**	**16h_up**	**0.0099**	**0.683**
transcription from RNA polymerase II promoter	GO:0006366	3h_up	0.0006	0.134
DNA modification	GO:0006304	3h_up	0.0008	0.134
response to cold	**GO:0009409**	**3h_up**	**0.0073**	**0.709**
organelle organization	**GO:0006996**	**3h_up**	**0.0083**	**0.709**

Supplemental Table 2: Primer used for qPCR

name	Sequence	name	Sequence 5´→ 3´
HDA8_f	AGCTGGTGGTTCCTGCAGTTA	**HD2A_f**	TGAGCCACAAGGCTATTCTGAGG
HDA8_r	AAAGCGCTAGAGTCTTGACCAAC	**HD2A_r**	AGCTACAGCCTTGGCAGCATTC
HDA19_f	TCTTGGGTGGTGGTGGTTACAC	**HD2B_f**	TGTTCCTGAAGCTGTTCCTGCTC
HDA19_r	TCCAAGTGCAACTCCAGTCTCG	**HD2B_r**	AACAGCTGCTCCAGCATTTCCG
HDA7_f	TCGTTGCTGGTGCTATGAGACG	**HD2C_f**	ACGACGAAGAAGATGACTCCTCAG
HDA7_r	ATTGCCTGGGAGATCATTGTCAAG	**HD2C_r**	CTCTTCTTGGGTTCTTCAGGCTTC
HDA9_f	ACTAGCCAGGGATCGACTAGGATG	**HD2D_f**	TCTTCTCAAGCAGCCACATCTTCC
HDA9_r	ATCCTCCACCTCCTGTAACCAG	**HD2D_r**	TCCCTGGCTTAATCTCGATACCC
HDA10_f	TCACAGGACATGCTGAATGTGG	**Srt1_f**	AGCTTTCTGAACTGCATGGAGAC
HDA10_r	AGTCTCAACGGTCCAACAACG	**Srt1_r**	ACCTCGAAATCACGCAGGTACTC
HDA14_f	ACCAACATATGCCACTTCAACGAC	**Srt2_f**	CCGCCATTAACGACCTCTCAAGTG
HDA14_r	ACTAAAGCCATTCCGGCTCCTG	**Srt2_r**	TTCGCGACGGAAACAAATCTGTAG
HDA5_f	TCCTGTGGCGAGGGAATTTAACC		
HDA5_r	CCTTGTGCAAACTCCATCAGCTTC		
HDA2_f	ACCCATTCCGAAAGCAGGTTGG		
HDA2_r	ATCGCCCATCCAAGTTCTGTTG		
HDA15_f	GATTTGATGCGGCTAGAGGAGACC		
HDA15_r	AATAGCCAGCCGGAGTCACATC		
HDA18_f	GCAGCTGGATCTGTTGTAAAGGTG		
HDA18_r	TCATCTGACTCGGCATGGTGTC		
HDA6_f	AACCTCGCATCTGGAGTGGAAC		
HDA6_r	ATCTTCACCGGTAGAGTCCCTGTC		

Supplemental Table 3: Primer used for ChIP-qPCR

name	Sequence	name	Sequence 5´→ 3´
Peak1_positive_f	TGCTACTCTCAATCCGACCC	**LHCB3_exon_f**	AACTCCGTCTTACCTCACCG
Peak1_positive_r	GTGAGGTGAAGAACAGGGGA	**LHCB3_exon_r**	TCAGGGTCTGCGGATAAACC
Peak1_negative_f	CACCTCTGCACAACCTTTCC	**ANTR1_exon_f**	GCGAATCAGAAACGACGTCA
Peak1_negative_r	TGGGAAACTGAGGCTTGTGA	**ANTR1_exon_r**	TCCGGGTATTAGTTCGGAGC
Peak2_positive_f	GCTGTGGATTGGTGGGTTTT	**At3g53830_exon_f**	TACTTACCAGGAGCTGCGTC
Peak2_positive_r	CAGACAACCCTTCAGCAACC	**At3g53830_exon_r**	GAATCCACAACCACCACCAC
Peak2_negative_f	TCTATGGAGAGAGGATTCGACG	**At1g62510_exon_f**	TTGGATGAGGGTGCAACATG
Peak2_neagtive_r	CGCACTCGTTTTGGGACTC	**At1g62510_exon_r**	CGGCCTACTAAACGTAACCC
Peak3_positive_f	GAGCTCCTCCAATGTGCAAG	**COL2_exon_f**	ACGAAGCAACCTCTCGATCA
Peak3_positive_r	GCTAATAGAAAGACGCCGCC	**COL2_exon_r**	TTCCGCAAACCCACTAGCTA
Peak3_neagtive_f	AAACCGATCGACCAAACCAC	**DOG1_exon_f**	CCCCACTCATGCATCGAAAG
Peak3_negative_r	CCAGTCTGTGCATTTCCAAGA	**DOG1_exon_r**	ACAAGGAGCGGATTTCTTGC

246

247
248
249

250

251

252

253

254

255

256

257

258

259

260

261

262
263

264